

## Accepted Manuscript

Sinkhole risk assessment by ERT: The case study of sirino lake (Basilicata, Italy)

V. Giampaolo, L. Capozzoli, S. Grimaldi, E. Rizzo

PII: S0169-555X(15)30164-1  
DOI: doi: [10.1016/j.geomorph.2015.09.028](https://doi.org/10.1016/j.geomorph.2015.09.028)  
Reference: GEOMOR 5395

To appear in: *Geomorphology*

Received date: 13 April 2015  
Revised date: 29 September 2015  
Accepted date: 30 September 2015



Please cite this article as: Giampaolo, V., Capozzoli, L., Grimaldi, S., Rizzo, E., Sinkhole risk assessment by ERT: The case study of sirino lake (Basilicata, Italy), *Geomorphology* (2015), doi: [10.1016/j.geomorph.2015.09.028](https://doi.org/10.1016/j.geomorph.2015.09.028)

This is a PDF file of an unedited manuscript that has been accepted for publication. As a service to our customers we are providing this early version of the manuscript. The manuscript will undergo copyediting, typesetting, and review of the resulting proof before it is published in its final form. Please note that during the production process errors may be discovered which could affect the content, and all legal disclaimers that apply to the journal pertain.

**Sinkhole risk assessment by ERT: the case study of Sirino Lake (Basilicata, Italy)****Giampaolo V.<sup>1</sup>, Capozzoli L.<sup>1</sup>, Grimaldi S.<sup>2</sup>, Rizzo E.<sup>1\*</sup>**<sup>1</sup>CNR-IMAA, Hydrogeosite Laboratory, Italy<sup>2</sup>University of Basilicata, Potenza, Italy

\*Corresponding author: enzo.rizzo@imaa.cnr.it

**Abstract**

The presence of natural or artificial lakes and reservoirs that can drain because of natural phenomena can generate catastrophic events affecting urban and agricultural areas next to the source area.

Therefore, geophysical prospecting techniques have been applied in the study of Sirino Lake, which, during the last century, was affected by the sudden opening of small sinkholes, resulting in the almost total draining of the lake and in the sudden increase of water flow rates of distal springs. Two electrical resistivity tomographies (ERT) were carried out across the lake, using electrode arrays located on land and across the water body. Self-potential (SP) data were acquired around the lake shore and the surrounding area. The geophysical prospecting contributed significant data toward explaining the unique hydrogeological characteristics of the lake. Integration of geophysical, geological, hydrogeological, and geomorphological data allowed us to estimate the thickness of the lacustrine deposits beneath the lake, to describe the main patterns of the subsurface fluid flows in the area, and to identify possible water escape routes causing the piping phenomena.

*Keywords:* piping; sinkhole; hydrogeology; ERT

## 1. Introduction

The presence of natural or artificial lakes and reservoirs that can empty because of natural phenomena such as landslides, flood, piping, and sinkhole formation is a serious hydrogeological problem because it can generate catastrophic events affecting urban and agricultural areas below the source area (Blown and Church, 1985; Meyer et al., 1994; Sammarco, 2004; Dai et al., 2005). The most common cause of natural dam failures are overtopping by a displacement wave created by debris avalanche into the lake, seepage erosion, slope instability, and earthquake-induced settlement or cracking (Awal et al., 2011; Moore et al., 2013). Seepage erosion phenomena are the cause of more catastrophic failures of engineered earth dams than any other mechanism except overtopping (Sherard et al., 1963). Anomalous seepage can create subsurface cavities that either release impounded water or collapse, lowering the dam crest (Moore et al., 2013).

In order to mitigate the erosion phenomena some fundamental questions is necessary answering regarding for example the thickness of the impermeable layer under the lake, the flow pathways, and the presence of possible water escape routes. The scientific community has therefore devoted considerable attention to geophysical methods suitable for identifying and mapping these features. Electrical resistivity tomography (ERT) and self-potential (SP) methods are relatively time and cost effective when working on large areas and are reasonably user-friendly for geomorphologists (Perrone et al., 2004; Lapenna et al., 2005; Naudet et al., 2008, Giampaolo et al., 2014).

The electrical resistivity method is an important tool in hydrogeological applications as the spatial distribution of electrical resistivity of the subsoil can provide important information that characterizes the heterogeneity of aquifers and sediments, reconstructs aquifers and/or aquiclude geometry and the relationships between freshwater and seawater, and estimates some hydrogeological parameters such as hydraulic head, porosity, water content, and hydraulic conductivity (Kosinski and Kelly, 1981; Daily et al., 1992; Slater et al., 1997; Binley et al., 2002; Dam and Christensen, 2003; Darnet et al., 2003; Binley and Kemna, 2005).

Presently the tomographic technique has become the most used geoelectrical technique form the high resolution of the large number of measurements and because of its execution speed, which results in considerable reduction of time and cost. The electrical resistivity survey methodology has been developed also to evaluate subsurface conditions under inundated areas (stream, river, wetland, lake, and sea) for hydrogeological and environmental purposes. Surveys in water-covered areas include conventional multielectrode resistivity surveys where part of the survey line crosses a river or a lake and surveys conducted entirely within an inundated environment (Loke and Lane, 2004). However, the geoelectrical method is better suited to dry land, and this method is not widely used in water-covered areas. Some authors have resorted to geoelectrical methods mostly in applications at sea or in rivers, where this method is performed with fixed electrodes placed on the water surface or on the sea and riverbed (De Souza and Sampaio, 2001; Kwon et al., 2005; Maillet et al., 2005; Freyer et al., 2006; Losito et al., 2007; Crook et al., 2008; Nyquist et al., 2008; Henderson et al., 2010; Orlando, 2013; Dahlin et al., 2014). Furthermore, the electric cable can be dragged on the water surface with the aid of ships or boats (Kwon et al., 2005; Day-Lewis et al., 2006; Castilho and Maia, 2008; Cardenas et al., 2010). In the first case, the cable is usually weighted in order to allow direct contact with the marine sediments (Henderson et al., 2010). The use of floating cables allows a wider area to be covered; however, measurement errors may be higher caused by stacking suppression, off-line array movement induced by boat navigation, wind or wave action, electrode cavitation at high boat speeds, and vegetation entrainment on electrodes (Day-Lewis et al., 2006). Usually, streamer electrodes are made of steel or graphite; however, the latter are more fragile but more resistant to saltwater corrosion (Day-Lewis et al., 2006).

Less common are electrical resistivity measurements in wetlands, ponds, and lakes. Examples of applications have been reported by Baumgartner (1996) who used electrodes located underwater and orientated vertically, Mansoor and Slater (2007) who performed aquatic electrical resistivity imaging to predict spatial and temporal patterns of pore-fluid conductivity in wetland soils using fixed floating electrodes, and Yang et al. (2006) who integrated GPR and resistivity image profiling

methods at the water surface. In the latter case, an electrode cable with electrodes at 1-m intervals and PVC bottles linked to each electrode to prevent the cable from sinking were used. Moreover, electrodes were kept in good contact with the water to ensure injection of electric current into the strata through the water. Finally, Befusa et al. (2014) investigated the Muri Lagoon of Rarotonga (Cook Islands) with a dense, multiscale network of electrical resistivity tomography (ERT) surveys using standard electrodes on land and across the foreshore, submerged electrodes in the shallow subtidal zone, and floating electrodes towed throughout the reef-surrounded lagoon by a boat.

Inversion algorithms generally used for inverting apparent electrical resistivity measurements in water-covered areas are commonly iterative, nonlinear, least squares methods, with regularization based on discretized first or second spatial derivative filters to produce a flat or smooth tomogram, respectively. As for land-based resistivity, inverse problems are underdetermined and tomograms should be considered low-resolution (i.e., blurry and blunted) versions of reality. One strategy to improve the resolution of electrical resistivity tomograms in water-covered areas is to incorporate constraints on the water-column resistivity and thickness (Loke and Lane, 2004; Orlando, 2013). In particular, the electrical resistivity of the water, within acceptable error margins can be considered constant.

The self-potential method (SP) is a passive geoelectrical technique, and it consists of measuring the potential differences between two nonpolarizable electrodes placed at the ground surface. These voltage differences result from the existence of an electric field produced by natural electrical sources distributed in the subsoil and generated by various phenomena (hydraulic, chemical, or thermal disequilibria). In particular, the SP method is sensitive to groundwater flow through the electrokinetic effect (Thony et al., 1997; Revil, 1999; Darnet and Marquis, 2004; Rizzo et al., 2004; Straface et al., 2007; Giampaolo et al., 2014). Therefore, detecting the electrokinetic effect based on the SP survey can allow zonation of infiltrating water recharge and runoff areas and can determine the extent of effects of subsurface drainage works. The SP map should describe the main patterns of

the subsurface fluid flow in clayey landslides, locating source and accumulation areas (Perrone et al., 2004, Naudet et al., 2008).

In this paper, we present a combined geophysical survey at Sirino Lake that had the objective of integrating previous surveys (Grassi et al., 2001b) and extending the depth in order to help solve the hydrogeological issue that affects Sirino Lake and the surrounding area (Nemoli, Basilicata). Historically, the lake has been intersected by many pipings as a result of sudden openings of small sinkholes (about 1-2 m in diameter) that resulted in almost total lake draining. Moreover, the hydraulic instability combined with the geomorphological and seismic risks characterise the entire area as potentially being exposed to flood and landslide risk caused by new episodes of pipe collapse and sinkhole formation.

## **2. Geological and hydrogeological setting**

Sirino Lake (Fig. 1), lying at 784 m asl (above sea level) is a major tourist site in the middle of an interesting natural area, between the towns of Lauria, Lagonegro, and Maratea (Basilicata region, Italy). Almost elliptical in shape, the lake covers about 3 ha with a 300-m length and 150-m width. The depth varies according to the season, but it does not exceed 6 m.

The lake lies on the SE side of the Sirino Mountain tectonic window at the base of the Costa del Capraro ridge. The area is underlain by a calcareous–siliceous marly succession attributable to Lagonegro I unit (M.Triassic-L.Cretaceous), which constitutes the backbone of Sirino Mountain. Lagonegro I unit terrains originated from the deformation of Lagonegro basin sediments during the tectonic phases that led to the building of the Apennines during the Tertiary (Scandone, 1972; Catalano et al., 2003; Butler et al., 2004). The terrains that crop out in the area consists of the following, from the bottom upward:

- Cherty Limestone Fm (*Calcari con selce*): dolomitic limestones with flint bands and cherty nodules (upper Triassic), overlain by;
- Siliceous Schists Fm (*Scisti Silicei*): multicoloured radiolarites and cherts, jaspers, siltites, and red and green-grey shales and marls (upper Jurassic-upper Triassic), overlain by;
- Flysch Galestrino Fm: argillites, shales and marls, and dark-grey siliceous limestones (lower Cretaceous-upper Jurassic).

These terrains are bounded by the Lagonegro II unit to the north, the Liguride and Carbonate Platform units to the east, the Liguride unit to the south, and Carbonate Platform units to the west (Fig. 2). Finally, massive glacial debris accumulations related to the last Wurm glacial phase and slope and/or landslide debris are present in the area (Guerricchio and Melidoro, 1981; D'Ecclesiis et al., 1990; Boenzi and Cherubini, 1993). From a structural point of view, the Sirino Mountain forms a brachyanticline, with the axis oriented roughly N-S, and made structurally more complex by a series of secondary folds and direct faults. The fold core consists, in the higher portions of the massif, in the oldest terrain (Flinty Cherty Limestone Fm) on which are, at intermediate altitudes, the Siliceous schists (Fig. 2). All around the nucleus outcrops the Flysch Galestrino Fm (Bonardi et al., in prep.).

The landscape surrounding the lake is characterized by a complex topography, mostly steep mountains that have historically been affected by large landslides, involving important infrastructure, such as the main highway of southern Italy (A3, SA-RC) and, immediately downstream of it, routes SS19 and SS104 (Guerricchio and Melidoro, 1981). The mass movements involve an area of several hundred acres, with the sliding surfaces above 40 m depth. Moreover, the displacements detectable on the surface are of the order of centimetres for the highway, several decimetres for the SS19, and some meters for the former SS104. Moving progressively toward the valley, the landslide evolution is typical of a rapid earthflow (Guida and Siervo, 2005; Guida et al., 2006; Bentivenga et al., 2010). Grassi et al. (2001b) described the geomorphology of the area near

Sirino Lake as characterized by different landslide types, and depending on the lithologies involved, at different altitudes. Translational landslides have produced large volumes of medium to large debris (late Pleistocene-Holocene) at the base of the slope, continuous rockfalls caused by the detachment of rock masses, leading to the continuous retreat of landslide scarps. These scarps delineate areas that constitute the catchment of some medium-sized rotational landslides. Debris, mostly made up of stone fragments of calcareous or siliceous nature (grain size of decimetres) with a disorganized structure, accumulated up to a height of 750 m asl, for a longitudinal runout of about 1400 m. From about 875 m asl, on the eastern side of Sirino Lake, the debris flowed onto deposits from a previous accumulation.

The studied area is entirely situated within the left bank valley slopes of the Noce River catchment. The surface drainage is poorly developed on outcropping permeable substrate sediments; on the contrary, it is better developed in areas underlain by clayey sediments in the northeastern zone.

The cherty limestone and siliceous schists are the main reservoir of the Sirino Mountain aquifer system. The cherty limestone is characterized by moderately high hydraulic conductivity, mainly caused by the widespread jointing and/or layering and to the major fracture systems oriented N-S and NNE-SSW. The siliceous schists, which are exposed on a dip slope, can be appreciably more permeable along the stratification planes and/or along bands of intense fracturing.

The system is variably buffered by a belt of soil with lower hydraulic conductivity soils (Flysch Galestrino Fm) that constitute the main aquiclude of the carbonate aquifer formed by Sirino Mountain (D'Ecclesiis et al., 1990). Locally, the siliceous schists act as an impermeable aquiclude (Grassi et al., 2001a). Moreover, in this formation the presence of shale levels and the alteration and fracturing effects can significantly increase the presence of low permeable soils.

The main system of faults are oriented N-S, influencing the whole groundwater flow within the rock mass favouring the outflow to the existing springs on the S-SW slope of Sirino Mountain. These springs are among the most abundant of the entire aquifer system. In the Sirino Lake source area, the waters discharge mainly at the contact between Siliceous Schists Fm and the Flysch Galestrino



Fm. The Sirino Lake surface water body is fed by perennial springs at 790 m asl that emerge from the aquifer circulating inside Sirino Mountain (*Sorgente del Lago*). The source area is a few hundred square meters wide where springs converge forming a small stream that flows into the lake. The spring discharge is about 130 l/s. Moreover, distal from the lake, two springs (*Sorgente Sotto il Lago I and II*) occur at 710 and 725 m asl (Fig. 2), with an average flow rate of about 2-3 L/s and 100 L/s, respectively.

Sirino Lake is a natural feature, although different interpretations of its genesis are available. De Lorenzo (1904) argued that its origin is glacial, while for other authors its genesis is linked to the evolution of a large landslide that involved the upstream of the lake (Guerricchio and Melidoro, 1981; Boenzi and Cherubini, 1993; Grassi et al., 2001b; ISPRA, Servizio Geologico d'Italia, 2014). Bentivenga et al. (2011) argued that Sirino Lake formed within a tectonic depression (syncline) fed by the Sirino spring.

In the last century, Sirino Lake was affected by the formation of many pipes, with a result of sudden openings of small sinkholes caused by pipe collapse, which resulted in almost the total lake draining. For these reasons, a series of local sealing remediation actions were carried out, without ever tackling the actual causes. The first consolidation efforts were made in the 1960s, by the laying of a sheath of asphalt on the lake shores and the construction of a weir as an artificial outlet. These measures, however, did not prevent the phenomenon from recurring at different times and in adjacent areas. The artificial structures have a negative environmental impact and are visually intrusive. The opening of these sinkholes is not predictable, and although draining events have been recorded since the early twentieth century, no written record of all the events are reported.

Among the most recent episodes, those that occurred in summer 2009 (Fig. 1C), 2011 (Lovoi, 2011), 2012 (Coppola et al., 2013), and 2014 (Fig. 1D) have been recorded. In July 1994, a 1-m-wide sinkhole opened in the SW side of the lake, about 3 m from the shore (Fig. 1B). The water flowing into the hole lowered the lake level about 2 m. Simultaneously, a sudden increase in the discharge of underlying spring sources occurred, in particular the *Sotto il Lago II* source spring

reached a discharge value of about 300 L/s. The piping stopped naturally following the collapse of a section of shoreline, with the consequent closure of the hole and the return (after a few days) to normal flow rates values (Grassi et al., 2001b).

Generally, episodes occur in the summer, and sinkholes open on the same shore that was affected in the 1994 episode, a few tens of meters away. In some cases, the holes were closed artificially with concrete.

### 3. Geophysical surveys

In order to investigate Sirino Lake and to delineate possible water escape routes under the lake or along the lake shores, two different types of geophysical methods were employed: two electrical resistivity tomographies (ERT) crossing the lake and along the lake shore and a self-potential (SP) survey of the surrounding area (Fig. 3). The geophysical results were compared with previous gamma ray data (Grassi et al., 2001b). It is a method of measuring naturally occurring gamma radiation, expressed in counts per minute (cpm), to characterize the rock or sediment in a borehole or drill hole; and it is performed by lowering a detector down the drilled hole and recording gamma radiation variation with depth. The log stratigraphy shows, in the first 6-7 m, the presence of reddish scaly clay containing sharp-edged clasts of a calcareous or siliceous nature.

#### 3.1. Electrical resistivity tomography survey

In July 2009, an electrical resistivity survey was carried out on land and on water to study the sinkhole phenomena along the Sirino Lake shores and to analyse the state of health of the impervious layer under the lake (Fig. 3).

The geoelectrical tomographies were performed using the Syscal Junior georesistivity meter (IRIS Instrument) coupled to a multielectrode system, consisting of two multichannel cables at 24 channels with an electrode spacing of 10 m. For the geoelectrical data acquisition in water, the cable was floated on the lake surface by means of a series of PVC bottles equally spaced, and the Syscal

Junior was placed on board a small boat and held steady in the lake centre for the whole duration of measurements (Fig. 3A and 3B). For the ground measurements, standard stainless steel electrodes connected to the cable were used. The ERT1, acquired across the lake, was done using Wenner-Schlumberger (WS) and dipole-dipole (DD) arrays. This ER profile was carried out between the northwestern and the southeastern lake shores, with a total length of 450 m, of which 210 m extended into the lake with electrodes floating on the water surface. Furthermore, water electrical conductivity and lake bathymetry and temperature were measured along the ERT profile (Fig. 3C and 3D).

The ERT2, carried out along the southern lake shore perpendicular to ERT1, was acquired using a dipole-dipole array in order to define the subvertical structures and with an electrode spacing of 10 m.

The apparent resistivity data were analysed and converted in real resistivity values by the inversion software ZondRes2D (Zond geophysical software), which is a computer program for 2.5D interpretation of electrical resistivity tomography. The first step was to prepare the data for the inversion, such as poor data detection. The next step was to select the inversion type and parameters. In order to transform the apparent resistivity pseudosection into a model representing the distribution of calculated electrical resistivity in the subsurface, we used the Occam method, which is an inversion by least-square method with the use of a smoothing operator and an additional contrast minimization (Constable et al., 1987). Moreover, all the resistivity data were inverted taking into account the topography. Water electrical resistivity and bathymetry constraints were included in the inversion processes, using a distorted finite element grid where the upper part of the mesh was used to model the water layer at the assigned electrical resistivity value of 40  $\Omega\text{m}$ , which was measured by an electrical conductivity meter at different depths down to 2.5 m from the water surface (Fig. 3D). The smoothness method adjusts the two-dimensional resistivity model trying to iteratively reduce the difference between the calculated and measured apparent resistivity values. The root mean-squared (RMS) error provides a measurement of this difference. The ERT1 was

acquired with different electrode arrays (DD and WS arrays) across even though they were expecting a better image from the combination of the two arrays. However, the results were similar, and no improvement in using two different acquisition configurations was achieved. In all cases, the RMS error ranged from 2.2% for WS to 7.9% for DD.

Although the two ERTs acquired with different arrays show similar results, some discrepancies were observed from the different approaches. The WS method provide more detail in the vertical plane while subvertical structures are resolved better by the DD technique. The electrical resistivity tomographies (Fig. 4) are characterized on the surface by relatively low electrical resistivity values ( $<100 \text{ Ohm}\cdot\text{m}$ ) down to 30 m deep and by higher electrical resistivity values ( $>500 \text{ Ohm}\cdot\text{m}$ ) at greater depth. On the NE part, the ERTs show a surface low resistivity zone connected to the electrical conductive electro-layer of the lake that crosses the underlying resistive body. In the SW zone, the two ERTs highlight complementary characteristics: the WS ERT (Fig. 4A) defines a resistive continuous layer extending from the NE, interrupted by a relatively conductive layer around 100 m from the start of the profile line. Conversely, the DD ERT (Fig. 4B) highlights the presence of a continuous resistive layer from the NE, but the zone between 80 to 180 m from the profile origin shows more lateral variation of the deep resistive layer.

Figure 5A defines the ERT2 carried out along the lake shore, perpendicular to the previous one. The electrical image shows a main deeper conductive electro-layer ( $<100 \text{ Ohm}\cdot\text{m}$ ) and localised discontinuous resistive zones ( $>500 \text{ Ohm}\cdot\text{m}$ ). The RMS error was 4.5%. The correlation between gamma ray log information and the first 30 m of ERT2 (Fig. 5B) shows clear alternations between levels: still plenty of clay characterized by low resistivity values and layers poor in clay matrix down to -24 m with a more resistive behaviour. In the deeper part, the gamma ray log shows the presence of a different lithotype poor in clay matrix probably correlated with landslide debris of the Siliceous Schist Formation (Fig. 5B). From a geophysical point of view, the ERT1 and ERT2 highlight the strong heterogeneity of the investigated area, closely correlated with the large number of landslides involving this flank of the Sirino Mountain.

### 3.2. Self-potential map

The self-potential (SP) method carried out in October 2010 allowed the analysis of the spatial-temporal dynamic of the electric charge distribution in the subsurface relative to groundwater flow. The water flow from upstream to downstream produces an accumulation of negative charges upstream and an accumulation of positive charges downstream. Therefore, this method can provide information on the movement of water and the preferential groundwater pathways.

In particular, electrical potential gradients (for a total of 226 measurement points) were measured along closed loops and profiles by alternating the leading and following electrodes (leap-frog technique) in order to reduce cumulative errors caused by electrode polarization. The distance between the measuring electrodes was 25 m. The SP values in the measuring net were obtained by adding readings after establishing an SP arbitrary zero value as a point of reference in the area. Moreover, SP measurements were corrected in order to compensate for cumulative errors. This is done by distributing the closure errors linearly along each circuit. In order to obtain a better visualization of the SP anomalies, we subtracted the net average value of the whole set of SP data from the potential obtained in each point.

Analysing the topography and SP trends for each measuring station, a correlation was observed between the two data sets. The SP measurements were corrected in order to compensate for the topographic effect. In general, a negative correlation between altitude and SP value along a slope is identified (Jackson and Kauahikaua, 1987; Sasai et al., 1997). The SP map, obtained using a contour line representation (Fig. 6), shows negative values upstream (down to -350 mV), while positive values (up to 150 mV) are present in the lower area surrounding the lake.

#### 4. Discussion of the results

The comparison between the electrical resistivity data, the geological maps and the results of a gamma-ray log previously carried out on the lake shore (Grassi et al., 2001b) allow us to reconstruct the complex geological section beneath Sirino Lake (Fig. 7). The elaborated geophysical data of profile AB (derived from ERT1) suggests that the shallow body with low electrical resistivity represents the lacustrine and shallow debris deposits beneath the lake bed that are characterized by inhomogeneous downward infiltration with high hydraulic permeability. The maximum thickness is reached in the lake centre where lacustrine deposits are about 30 m thick. The deeper resistive area denotes the presence of a zone of low fracturing density of the siliceous schists landslide debris and a generally low-medium hydraulic conductivity. The ERT1 (profile AB) underlines the presence of a low resistivity area, close to the lake shore on the SW portion, interpreted as a highly fractured zone within the siliceous schists debris and characterised by high hydraulic conductivity. The ERT2 (profile CD) also defined a large fractured zone along the lake shore. This area, connected with the shallower permeable sediments under the lake, may represent a possible water escape route because it is characterized by more permeable layers that overlie the less permeable shale and marl deposits of the Flysch Galestrino Fm.

Based on the analysis of SP data (Fig. 6), the Sirino Lake proximal area is characterized by negative electrical potential values (blue). This is caused by the higher permeability of the debris present on the slope, which allows water to flow downward. In the central part of the lake basin, we observed positive electrical potential values (red) representing the area of maximum water storage. In the distal lake area, a concentration of negative electrical potential values is again observed indicative of a water flow toward the lower area. The area where the *Sotto il Lago I* and *II* springs are present is characterised by negative electrical potential. This is clearly only a qualitative description of the SP anomaly field. We lack detailed information on the local hydrogeological setting and hydraulic parameters. Moreover, we do not yet have direct measurements of the  $\zeta$  potential, which is a key

parameter of electrokinetic phenomena (Revil, 1999), as well as a significant theoretical basis for the evaluation of the correlation between charge accumulations and local hydrogeological settings.

The interpretation and analysis of the geophysical surveys results allowed the precise identification of an underground area, located immediately downstream of the lake (SW). On the southern shore, ERTs and the gamma-ray log underline the presence of permeable sediments where water infiltration is directed. The concentrated flow processes are associated with the translocation of the finer fractions that give rise to small collapses of the underground pipes (piping sinkholes) with a return period randomly variable (generally multiyear).

Natural erosive pipes are formed near the left bank of the lake where the groundwater flow is evidently concentrated because of the presence of more permeable sediments. Headward erosion of the piping sinkholes and collapse beneath the bed of the southern shore of the lake leads to the opening of sinkholes that are able to accommodate water flow on the order of 100 L/s.

Siphoning episodes are, therefore, largely determined by a strong hydraulic gradient between the water level of the lake and the distal zone (SW) during rapid draining events. These spring sources (*Sotto il Lago I and II*), represent discharge from the aquifer through transmissive zones in the fractured siliceous schist debris and supported by marl on which the schists rest. The aquifer is probably fed by the discharge of the surface water body and the perched aquifer that lies in the detritus layer. An additional water supply could come from the aquifer circulating within the cherty limestone and siliceous schists that form the backbone of Sirino Mountain.

The geophysical data give us some new elements that confirm the hypothesis that the Sirino Lake depression may be generated by landslide phenomena and that the well-localized seepage zone could strongly contribute to piping phenomena suddenly occurring below the lake. Finally, the ERT images show the presence of fragmented high electrical resistivity blocks chaotically immersed inside a high conductivity matrix along the southern shore of the lake, indicative of allochthonous debris.

## 5. Conclusions

The different geoelectrical prospecting methods combined with geological, geomorphological, and borehole data allow us to interpret the unique hydrogeological characteristics of the Sirino lake area. The integrated results define the geometry of the landslide that formed the Sirino Lake depression in the past and the thickness of the lacustrine deposits under the lake. The most important result is the delineation of the susceptible sediments characterised by claimable piping phenomena.

The electrical resistivity tomographies highlight the possible water escape routes under the lake on the SW zone of the lake shore where piping and sinkhole collapse phenomena have occurred. This area is probably characterized by the presence of strongly jointed and fissured rocks (Siliceous Schists Fm landslide debris) made more permeable by the mechanism of seepage erosion. This phenomenon is particularly active when the water supply from the Sirino Mountain increases substantially. The self-potential survey allowed us to describe the main patterns of the subsurface fluid flows in the area, although the complexity of the situation does require more hydrogeological measurements to fully explain the periodic phenomenon.

We emphasize that the use of electrical resistivity measurements over water-covered areas, integrated with geological and hydrogeological investigations and geomorphologic information, can be a useful tool for investigating lake and wetland areas with complex hydrogeological features affected by seepage phenomena. The Sirino Lake seepage erosion could increase the water supply in the area and therefore could lead to destabilisation of unstable rock masses leading to landslides in the area.

In the future, using a monitoring strategy focused on the southern lake shore will help to better understand the time dynamics of the hydrogeological processes of instability phenomena that affect Sirino Lake that could predict sinkhole formation and avoid future lake-draining events and lake depletion.



**Acknowledgements**

The authors are grateful for the geological and logistical support of the Micromondo, the first theme park on geology, in order to create an impetus to the dissemination of knowledge concerning the Earth Sciences (geologists Patrizia Magnotti and Dario Rizzo, <http://www.ilmicromondo.com>). The authors thank Gregory De Martino and Antonella Lombardo for their help during the field work. Finally, the authors are grateful to Alex Kaminsky for the use of the inversion software ZondRes2D. The authors also thank the Editor and the referees for their helpful comments that strongly improve this manuscript.

ACCEPTED MANUSCRIPT

## References

- Awal, R., Nakagawa, H., Fujita, M., Kawaike, K., Baba, Y., Zhang, H., 2011. Study on Piping Failure of Natural Dam. *Journal of Japan Society of Civil Engineers* 67(4), 539-547.
- Baumgartner, F., 1996. A new method for geoelectrical investigations underwater. *Geophysical Prospecting* 44, 71–98.
- Befusa, K.M., Cardenas, M.B., Taitb, D.R., Elerb, D.V., 2014. Geoelectrical signals of geologic and hydrologic processes in a fringing reef lagoon setting. *Journal of Hydrology* 517, 508–520.
- Bentivenga, M., Giovagnoli, M.C., Palladino, G., Ruscito, V., 2010. Interazione fra infrastrutture lineari e patrimonio geologico. In *ISPRA - CATAP, Ambiente, paesaggio e infrastrutture. Volume I, Manuali e Linee Guidan.65/2010, ISPRA.*
- Bentivenga, M., Cavalcante, F., Palladino, G., Pansardi, N., 2011. Il lago Sirino e l'area del ponte delle ferrovie calabro-lucane di Lagonegro (Potenza): due geositi di interesse geologico e geomorfologico. *Geologia dell'ambiente SIGEA* 2/2011, 53-61.
- Binley, A., Kemna, A., 2005. Electrical Methods. **In: Rubin, Y. and Hubbard, S.S. (Eds.), Hydrogeophysics.** Springer , pp. 129-156.
- Binley, A., Winship P., West, L.J., Pokar, M., Middleton R., 2002. Seasonal variation of moisture content in unsaturated sandstone inferred from borehole radar and resistivity profiles. *Journal of Hydrology* 267, 160–172.
- Blown, I., Church, M., 1985. Catastrophic lake drainage within the Homathko River basin, British Columbia. *Canadian Geotechnical Journal* 22(4), 551-563, 10.1139/t85-075.
- Boenzi, F., Cherubini, C., 1993. Frane in roccia sul versante occidentale del monte Sirino in Basilicata. *Atti Soc. Tosc. Sc. Nat. Mem., XC*, 237-251.

- Bonardi, G., Cinque, A., De Capoa, P., Esposito, P., Guida, D., Mazzoli, S., Parente, M., Radoicic, R., Sgrosso, A., Siervo, V., Zamparelli, V., in prep. Note Illustrative della Carta Geologica d'Italia alla scala 1:50.000, Foglio 521 Lauria. APAT, Dipartimento Difesa del Suolo, Servizio Geologico d'Italia.
- Butler, R.W.H., Mazzoli, S., Corrado, S., De Donatis, M., Di Bucci, D., Gambini, R., Naso, G., Nicolai, C., Scrocca, D., Shiner, P., Zucconi, V., 2004. Applying thick-skinned tectonic models to the Apennine thrust belt of Italy—Limitations and implications. **In: McClay, K.R. (Ed.)**, Thrust tectonics and hydrocarbon systems. AAPG Memoir 82, 647– 667.
- Cardenas, M.B., Zamora, P.B., Siringan, F.P., Lapus, M.R., Rodolfo, R.S., Jacinto, G.S., San Diego -McGlone, M.L., Villanoy, C.L., Cabrera, O., Senal, M.I., 2010. Linking regional sources and pathways for submarine groundwater discharge at a reef by electrical resistivity tomography,  $^{222}\text{Rn}$ , and salinity measurements. *Geophysical Research Letters* 37, L16401.
- Castilho, G., Maia, D., 2008. A successful mixed land underwater 3D resistivity survey in an extremely challenging environment in Amazônia. 21th EEGS Symposium on the Application of Geophysics to Engineering and Environmental Problems, 1150-1158.
- Catalano, S., Monaco, C., Tortorici, L., Paltrinieri, W., Steel, N., 2003. Neogene-Quaternary tectonic evolution of the southern Apennines. *Tectonics* 23, doi:10.1029/2003TC001512.
- Constable, S.C., Parker, R.L., Constable, C.G., 1987. Occam's Inversion: a practical algorithm for generating smooth models from EM sounding data, *Geophysics* 52, 289-300.
- Coppola, L., Filardi, A., Bromhead, E.N., 2013. Landslide and flood hazard from the Lago Sirino, Basilicata, Italy. *Italian Journal of Engineering Geology and Environment* 6, 393-398, Book Series.

- Crook, N., Binley, A., Knight, R., Robinson, D. A., Zarnetske, J., Haggerty, R., 2008. Electrical resistivity imaging of the architecture of substream sediments. *Water Resources Research* 44, W00D13, doi:10.1029/2008WR006968.
- D'Ecclesiis, G., Grassi, D., Sdao, F., Tadolini, T., 1990. Potenzialità e vulnerabilità delle risorse idriche sotterranee del monte Sirino (Basilicata). *Geologia Applicata e Idrogeologia* 25, 195-219.
- Dahlin, T., Loke, M.H., Siikanen, J., Höök, M., 2014. Underwater ERT survey for site investigation for a new line for Stockholm metro. 20<sup>th</sup> European Meeting of Environmental and Engineering Geophysics Athens, Greece, 14-18 September 2014.
- Dai, F.C., Lee, C.F., Deng, J.H., Tham, L.G., 2005. The 1786 earthquake-triggered landslide dam and subsequent dam-break flood on the Dadu river, Southwestern China. *Geomorphology* 65, 205–221.
- Daily, W., Ramirez, A., Labrecque, D., Nitao, J., 1992. Electrical resistivity tomography of vadose water movement. *Water Resources Research* 28, 1429-1442.
- Dam, D., Christensen, S., 2003. Including geophysical data in groundwater model inverse calibration. *Ground Water* 41, 178-189.
- Darnet, M., Marquis, G., 2004. Modelling streaming potential (SP) signals induced by water movement in the vadose zone. *Journal of Hydrology* 285, 114–124.
- Darnet, M., Marquis, G., Sailhac, P., 2003. Estimating aquifer hydraulic properties from the inversion of surface Streaming Potential (SP) anomalies. *Geophysical Research Letters* 30, doi: 10.1029/2003GL017631.
- Day-Lewis, F.D., White, E.A., Johnson, C.D., Lane, J.W.JR., Belaval, M., 2006. Continuous resistivity profiling to delineate submarine groundwater discharge—examples and limitations. *The Leading Edge*, June 2006, 724-728.

- De Lorenzo, G., 1904. Geologia e geografia fisica dell'Italia meridionale. Laterza, Bari.
- De Souza, H., Sampaio, E.E.S., 2001. Apparent resistivity and spectral induced polarization in the submarine environment. *An. Acad. Bras. Cienc.* 73 (3), 429-444.
- Freyer, P. A., Nyquist, J. E., Toran, L. E., 2006. Use of underwater resistivity in the assessment of groundwater-surface water interaction within the burd run watershed. In *Proceedings of the Annual Symposium on the Application of Geophysics to Engineering and Environmental Problems*, 8. Seattle, Washington: Environmental and Engineering Geophysical Society.
- Giampaolo, V., Rizzo, E., Titov, K., Konosavsky, P., Laletina, D., Mainault, A., Lapenna V., 2014. Self-potential monitoring of a crude oil contaminated site (Trecate, Italy). *Environ Sci Pollut Res* 21, 8932–8947 DOI: 10.1007/s11356-013-2159-y.
- Grassi, D., Grimaldi, S., Sdao, G., Spilotro, G., 2001a. Ambiente idrogeologico e fenomeni di sifonamento relativi al Lago di frana Sirino (Basilicata). *Atti del convegno Geoitalia 2001*, 320-322, Chieti.
- Grassi, D., Grimaldi, S., Sdao, G., Spilotro, G., 2001b. Geologia, geomorfologia, idrogeologia e stabilità idraulica del lago Sirino (Basilicata). *Atti del Dipartimento Strutture, Geotecnica, Geologia Applicata all'Ingegneria - Università della Basilicata* 3, 20 pp, Lamisco-Spes, Potenza.
- Guerricchio, S., Melidoro, G., 1981. Movimenti di massa pseudotettonici nell'Appennino dell'Italia Meridionale. *Geol. Appl. e Idrog.*, vol. XVI, Bari.
- Guida, D., Siervo, V., 2005. La Carta Inventario dei Fenomeni Franosi del Foglio 521" Lauria". *Giornale di Geologia Applicata* 2, 58-64.
- Guida, D., Nocera, N., Siervo, V., 2006. Analisi morfoevolutiva sulla riattivazione di sistemi franosi a cinematiso intermittente in Appennino campano-lucano (Italia meridionale). *Giornale di Geologia Applicata* 3, 114-122.

- Henderson, R.D., Day-Lewis, F.D., Abarca, E., Harvey, C.F., Karam, H.N., Liu, L., Lane, J.W., 2010. Marine electrical resistivity imaging of submarine groundwater discharge: sensitivity analysis and application in Waquoit Bay, Massachusetts, USA. *Hydrogeology Journal* 18, 173–185.
- ISPRA, Servizio Geologico d'Italia – 2014. Lauria Foglio 521 della Carta 1:50.000 dell'IGM.
- Jackson, D.B., Kauahikaua, J., 1987. Regional self-potential anomalies at Kilauea volcano. *Volcanism in Hawaii*. USGS Professional paper 1350(40), 947–959.
- Kosinski, W.K., Kelly, W.E., 1981. Geoelectric soundings for predicting aquifer properties. *Ground Water* 19, 163-171.
- Kwon, H., Kim, J., Ahn, H., Yoon, J., Kim, K., Jung, C., Lee, S., Uchida, T., 2005. Delineation of fault zone beneath a riverbed by an electrical resistivity survey using a floating stream cable. *Exploration Geophysics* 36, 50-58.
- Lapenna, V., Lorenzo, P., Perrone, A., Piscitelli, S., Rizzo, E., Sdao, F., 2005. 2D Electrical Resistivity Imaging of some complex Landslides in Lucanian Apennine (Southern Italy). *Geophysics* 70(3), B11-B18.
- Loke, M.H., Lane, J.W., 2004. Inversion of data from electrical resistivity imaging surveys in water-covered areas. *Exploration Geophysics* 35, 266-271.
- Losito, G., Aminti, P.L., Martelletti, L., Grandjean, J.-M., Mazzetti, A., Trova, A., Benvenuti, G., 2007. Marine geoelectrical prospecting for soft structures characterization in shallow water: field and laboratory test. EAGE 69th Conference & Exhibition — London, UK, 11 - 14 June 2007.
- Lovoi, S., 2011. Una voragine sta prosciugando il lago Sirino.  
<http://www.lagazzettadelmezzogiorno.it/notizia.php?IDNotizia=444544&IDCategoria=12>  
accessed 23rd December 2012.

- Maillet, G., Rizzo, E., Revil, A., Vella, C., 2005. High resolution ERT applied in sand-bed channel mouth infilling. The test site of Pégoulie channel in the Rhône Delta, France. *Marine Geophysical Research* 26(2-4), 317-328
- Mansoor, N., Slater, L., 2007. Aquatic electrical resistivity imaging of shallow-water wetlands. *Geophysics* 72, F211–F221.
- Meyer, W., Schuster, R. L., Sabol, M. A., 1994. Potential for seepage erosion of landslide dam. *Journal of Geotechnical Engineering* 120, 1211–1229.
- Moore, J.R., Boleve, A., Sanders, J.W., Glaser, S.D., 2013. Self-potential investigation of moraine dam seepage. *Journal of Applied Geophysics* 74, 277–286.
- Naudet, V., Lazzari, M., Perrone, A., Loperte, A., Piscitelli, S., Lapenna, V., 2008. Integrated geophysical and geomorphological approach to investigate the snowmelt-triggered landslide of Bosco Piccolo village (Basilicata, southern Italy). *Engineering Geology* 98, 156–167.
- Nyquist, J.E., Freyer, P.A., Toran, L., 2008. Stream bottom resistivity tomography to map ground water discharge. *Ground Water* 46(4), 561–569.
- Orlando, L., 2013. Some considerations on electrical resistivity imaging for characterization of waterbed sediments. *Journal of Applied Geophysics* 95, 77–89.
- Perrone, A., Iannuzzi, A., Lapenna, V., Lorenzo, P., Piscitelli, S., Rizzo, E., Sdao, F., 2004. High-resolution electrical imaging of the Varco d'Izzo earthflow (southern Italy). *J. Appl. Geophys.* 56, 17–29.
- Revil, A., 1999. Ionic diffusivity, electrical conductivity, membrane and thermoelectric potentials in colloids and granular porous media: a unified model. *Journal of Colloid Interface Science* 212, 503–522.
- Rizzo, E., Suski, B., Revil, A., Straface, S., Troisi, S., 2004. Self-potential signals associated with pumping tests experiments. *Journal of Geophysical Research* 109, doi: 10.1029/2004JB003049.

- Sammarco, O., 2004. A Tragic Disaster Caused by the Failure of Tailings Dams Leads to the Formation of the Stava 1985 Foundation. *Mine Water and the Environment* 23, 91–95.
- Sasai, Y., Zlotnicki, J., Nishida, Y., Yvetot, P., Morat, P., Murakami, H., Tanaka, Y., Ishikawa, Y., Koyama, S., Sekiguchi, W, 1997. Electromagnetic monitoring of miyake-jima volcano, izu-bonin arc, japan: a preliminary report. *Journal of Geomagnetism and Geoelectricity* 49, 1293–1316.
- Scandone, P., 1972. Studi di geologia lucana: carta dei terreni della serie calcareo-silicomarnosa e note illustrative. *Bollettino della Società dei Naturalisti* 81, Napoli.
- Sherard, J.L., Woodward, R.J., Gizienski, S.F., Clevenger, W.A., 1963. *Earth and Earth-Rock Dams*. John Wiley and Sons, New York, NY.
- Slater, L., Binley, A., Brown, D, 1997. Electrical imaging of fractures using ground-water salinity change. *Ground Water* 35, 436-442.
- Straface, S., Fallico, C., Troisi, S., Rizzo, E., Revil, A., 2007. An inverse procedure to estimate transmissivity from heads and self-potential signals. *Ground Water* 45, 420–428.
- Thony, J.L., Morat, P., Vachaud, G., Mouel, J.L.L., 1997. Field characterization of the relationship between electrical potential gradients and soil water flux. *Comptes rendus de l'Académie des Sciences de Paris Série Ila* 325, 317–321.
- Yang, C., Tong, L.T., Yu, C.Y., 2006. Integrating GPR and RIP Methods for Water Surface Detection of Geological Structures. *TAO* 17, 391-404.



**Figures**

Fig. 1. Sirino Lake (A) affected by piping phenomena in 2004 (B), 2009 (C) and 2014 (D).

Fig. 2. Schematic geological map and section modified from Bonardi et al. (in prep.).

Fig. 3. Electrical resistivity measurements at Sirino lake using floating and on land electrodes (A); the center of the ERT1 was placed at the center of the lake putting the georesistivity meter on a pedal boat (B). Lake bathymetry (C) and water lake electrical conductivity until 2.5 m deep (D).

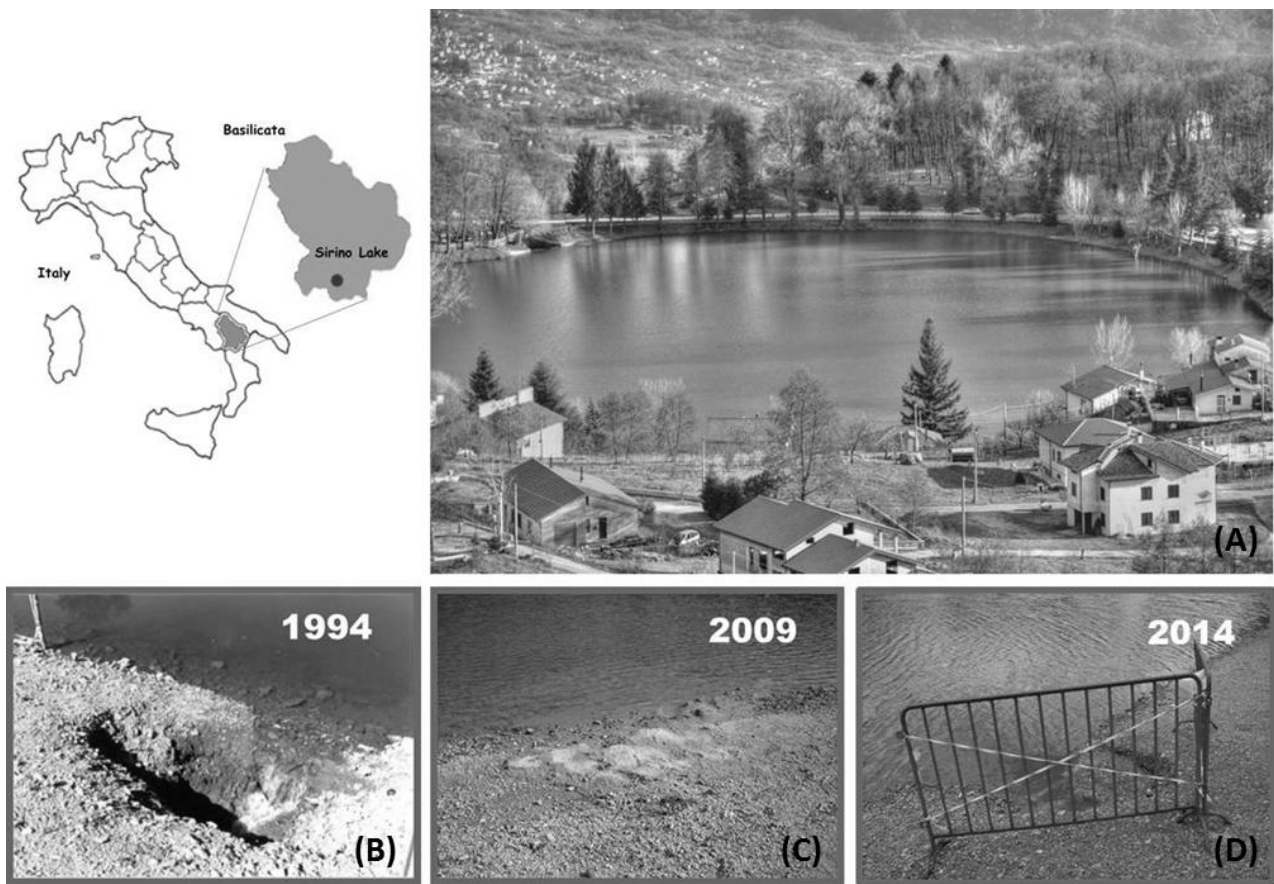
Fig. 4. ERT1 tomography acquired using Wenner-Schlumberger (A) and dipole-dipole (B) arrays. The dashed black line denotes lake bathymetry.

Fig. 5. (A) The ERT2 acquired using Dipole-Dipole array, carried out along the lake shore. The solid black line represents the gamma ray log; (B) gamma ray log reported by Grassi et al. (2001b).

Fig. 6. The self-potential map on the geological sketch and reconstruction of the main water flux direction.

Fig. 7. Geological interpretation of the ERT1 (AB) and ERT2 (CD). The symbols LP, LMP, and HP are (respectively) low hydraulic conductivity, low-medium hydraulic conductivity, and high hydraulic conductivity.

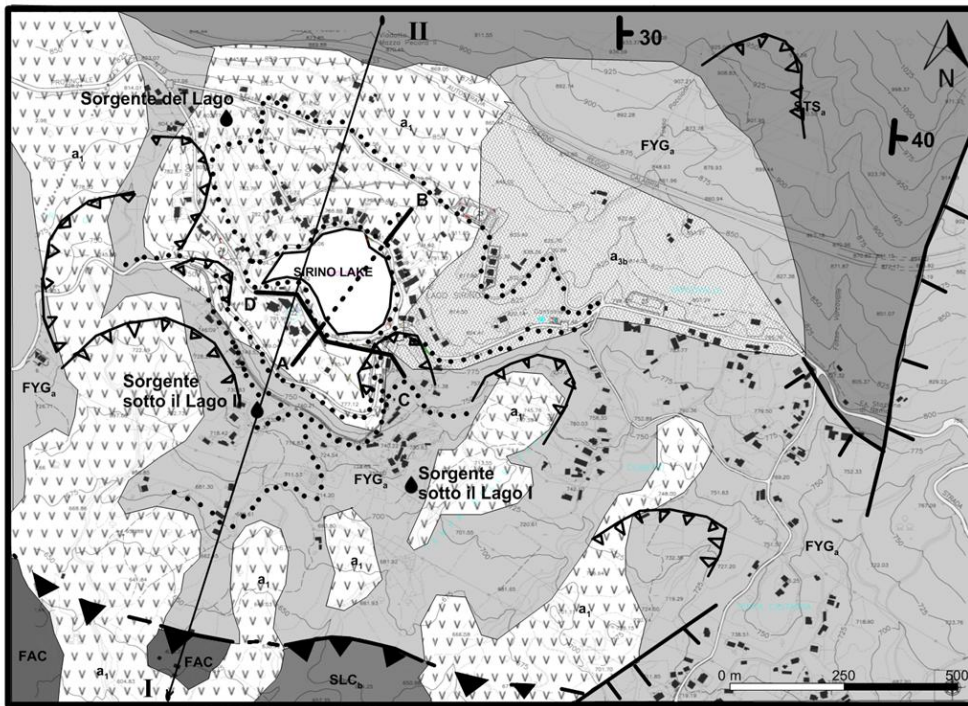
FIGURE 1



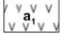






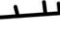


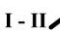






ACCEPTED

FIGURE 2

SIRINO LAKE GEOLOGICAL SCHEME



LEGEND

-  LANDSLIDES DEPOSITS
-  DEBRIS
- LAGONEGRO I UNIT**
-  FLYSCH GALESTRINO FM
-  SILICEOUS SCHISTS FM
- LAGONEGRO II UNIT**
-  CHERTY LIMESTONE FM
-  MONTE FACITO FM
-  STRATIGRAPHIC LIMITS
-  NORMAL FAULT
-  TRUST
-  TRUST, UNCERTAIN
-  STRIKE AND DIP
-  GEOLOGICAL PROFILE TRACE
-  LANDSLIDE SCARP
-  SOURCES
-  SP MEASUREMENTS POINT
-  ERT PROFILES (ELECTRODES ON LAND)
-  ERT PROFILE (ON WATER FLOATING ELECTRODES)

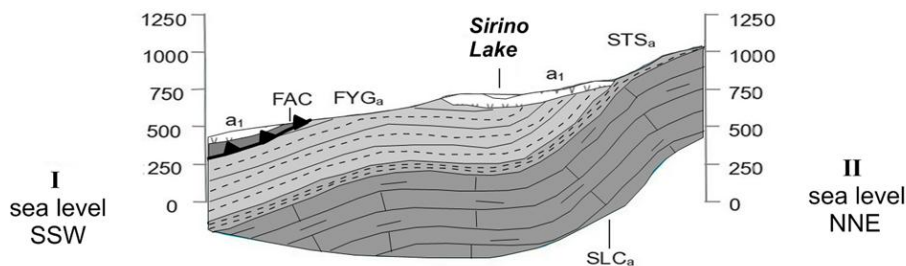
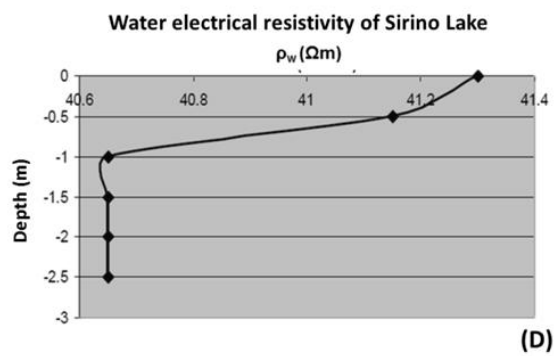
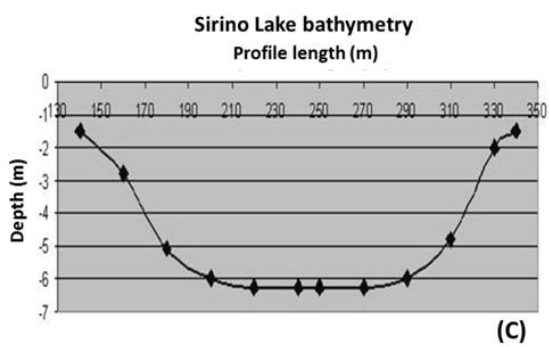


FIGURE 3



ACCEPTED

FIGURE 4

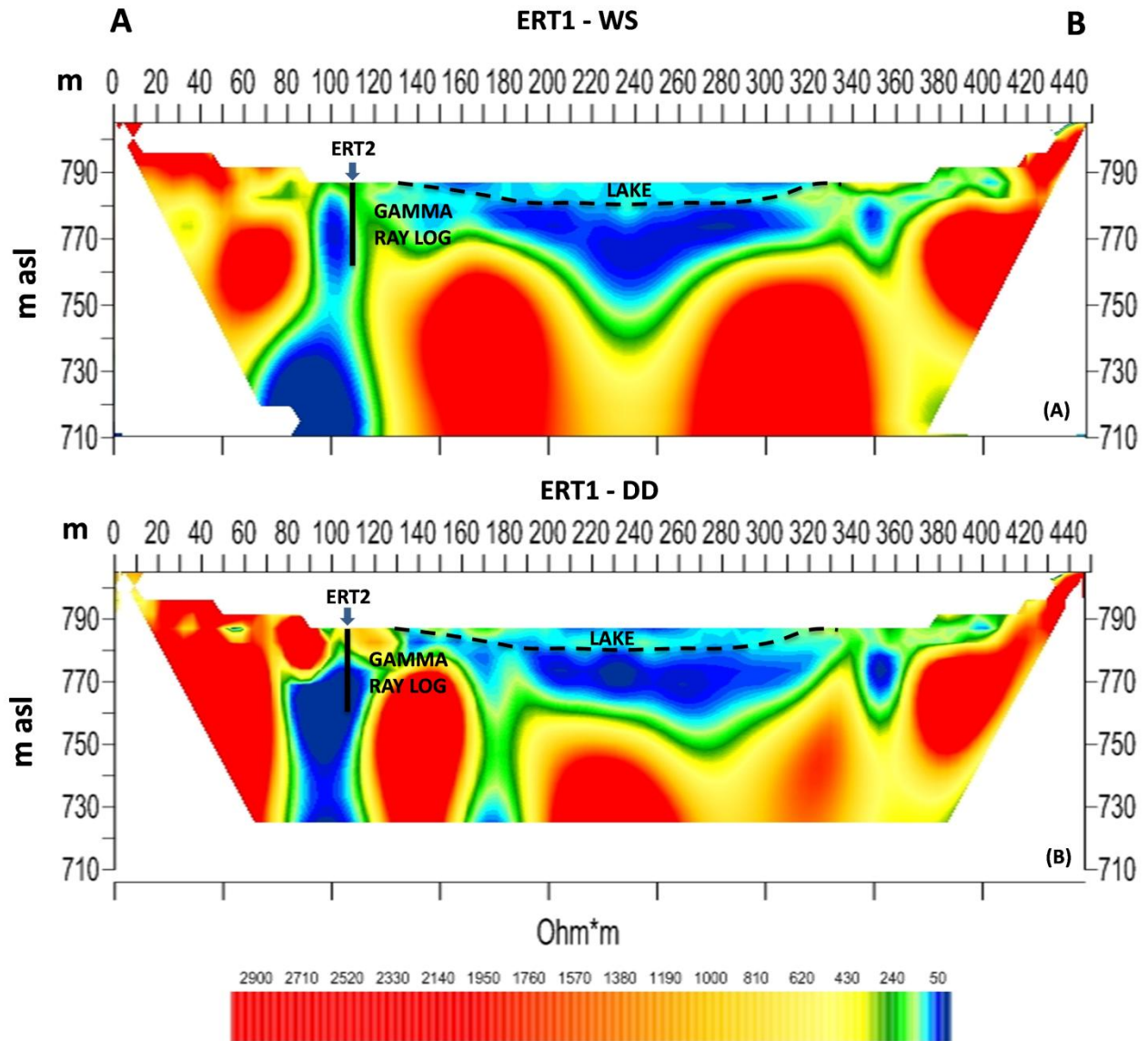


FIGURE 5

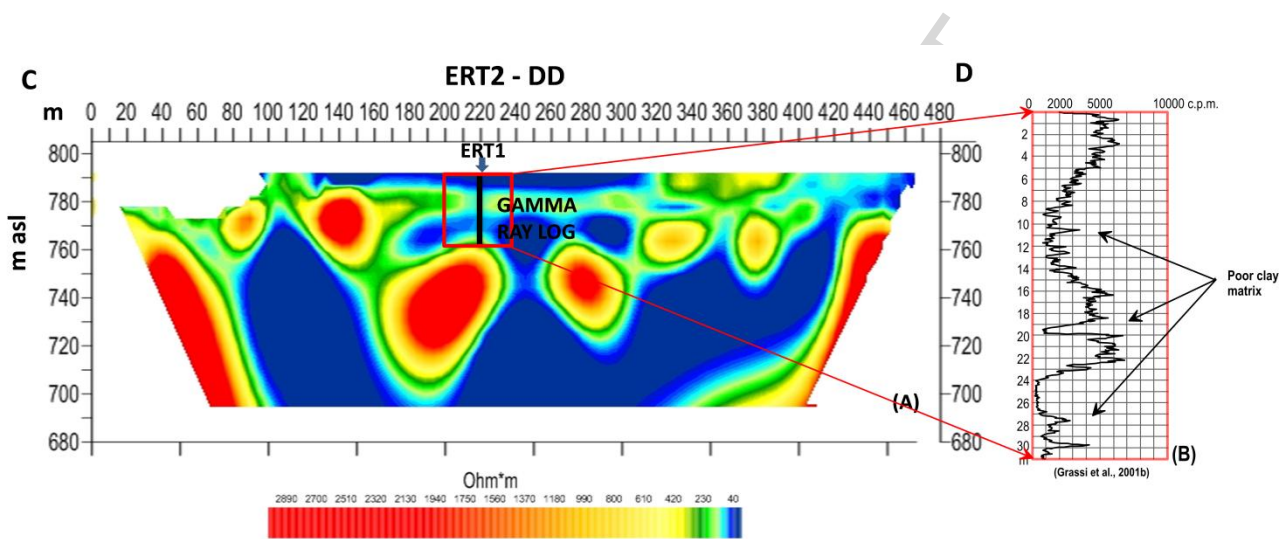


FIGURE 6

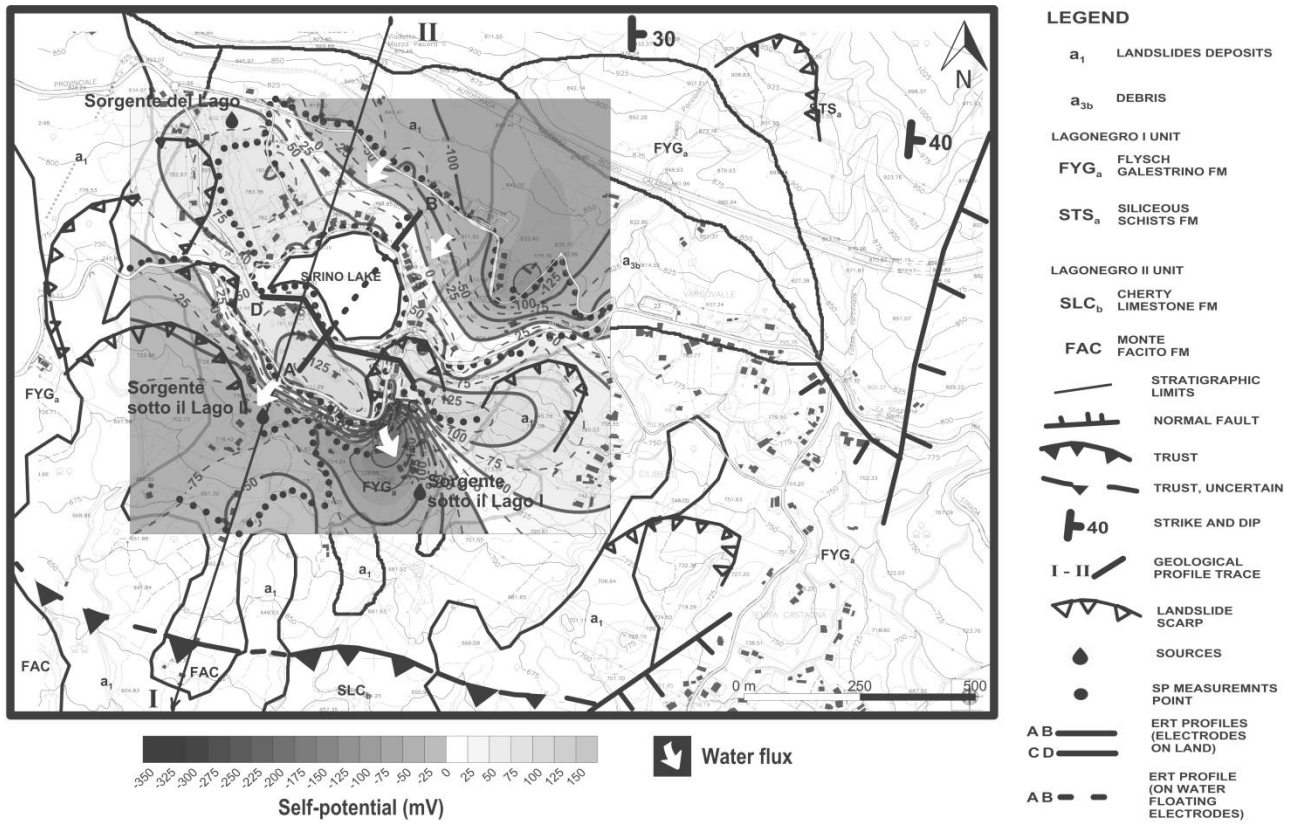
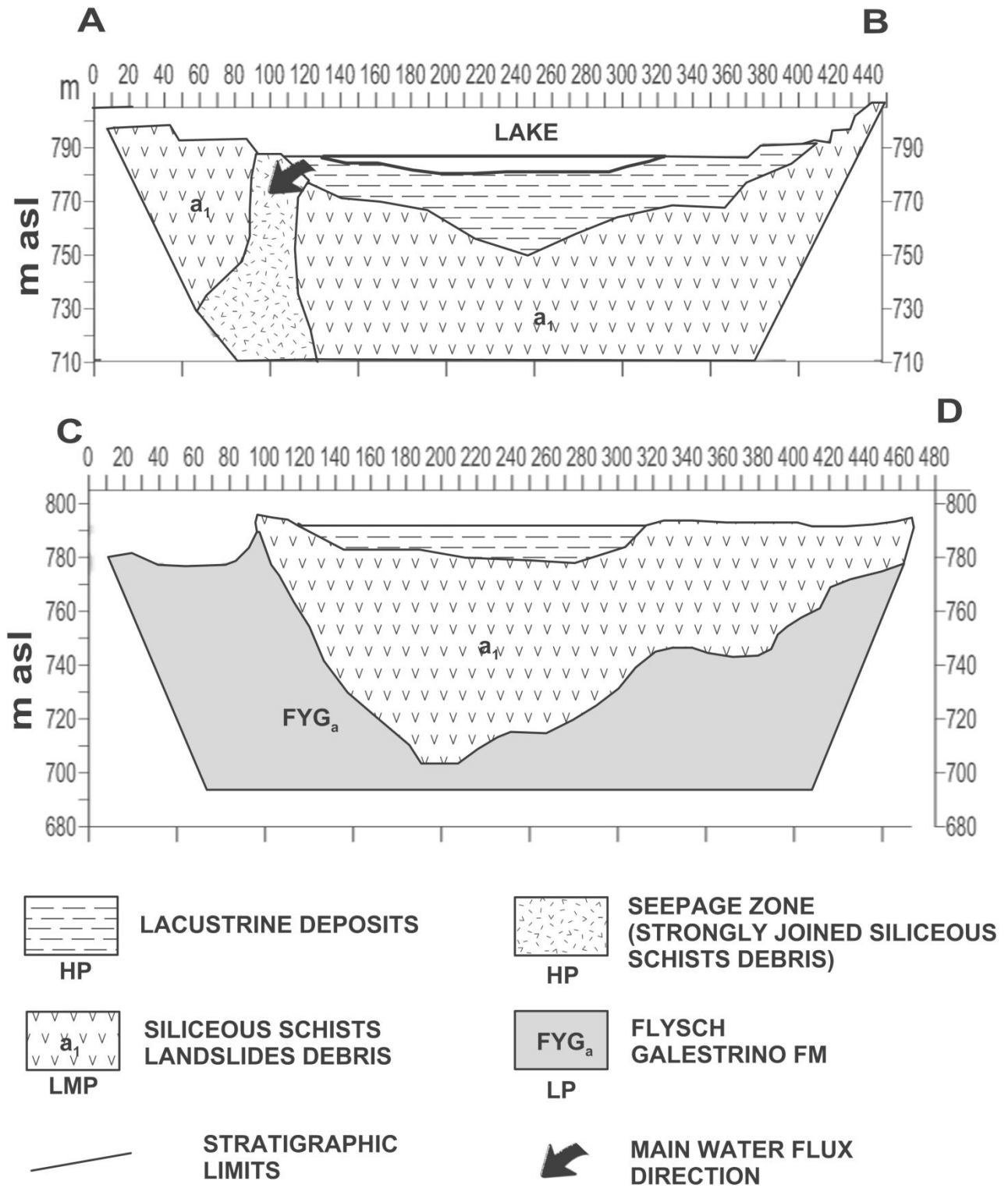


FIGURE 7





**Research highlights**

- ▶ We study the Sirino lake, affected by piping phenomena, by geophysics
- ▶ We integrate geophysical and hydro-geomorphological information
- ▶ The electrical resistivity tomographies individuate possible water escape routes
- ▶ We propose a monitoring system on the vulnerable lake shore

ACCEPTED MANUSCRIPT